Fountain Sam (Orcid ID: 0000-0002-6028-0548)

Maffia Pasquale (Orcid ID: 0000-0003-3926-4225)

Inhibitors of diacylglycerol metabolism suppress CCR2 receptor signalling in human monocytes

Day P[1], Burrows L[1], Richards D[1] and Fountain SJ[1,2]

[1]Biomedical Research Centre, School of Biological Sciences, University of East Anglia, Norwich, NR4 7TJ.

[2]Correspondence to s.j.fountain@uea.ac.uk

RUNNING TITLE DAG metabolism inhibitors suppress CCL2 signalling

AUTHOR CONTRIBUTION PD, LB and DR carried out the experiments and analysed the data. SJF designed the experiments and wrote the manuscript.

CONFLICT OF INTEREST The authors declare no conflicts of interest.

DECLARATION OF TRANSPARENCY AND SCIENTIFIC RIGOUR This Declaration acknowledges that this paper adheres to the principles for transparent reporting and scientific rigour of preclinical research as stated in the *BJP* guidelines for Design & Analysis, and Immunoblotting and Immunochemistry, and as recommended by funding agencies, publishers and other organisations engaged with supporting research.

BULLET POINT SUMMARY

What is already known: CCL2-mediated monocyte recruitment to tissue is involved in the onset and development of several chronic inflammatory diseases.

What this study adds: Pharmacological inhibition of DAG metabolism is a novel route to attenuate CCL2 signalling in human monocytes

Clinical significance: Possible novel therapies to inhibit unchecked monocyte tissue recruitment

ABSTRACT

Background and purpose
CCL2 is an inflammatory chemokine that stimulates the recruitment of monocytes into tissue via activation of the GPCR CCR2.

Experimental approach
Freshly isolated human monocytes and THP-1 cells are used; Fura-2 loaded cells used to measure intracellular Ca^{2+} responses; transwell migration; siRNA-mediated gene knockdown.

Key results
We observed that CCL2 evokes intracellular Ca^{2+} signals and stimulates migration in THP-1 monocytic cells and human CD14$^+$ monocytes in a CCR2-dependent fashion. Attenuation of diacylglycerol (DAG) catabolism in monocytes by inhibiting DAG kinase (R59949) or DAG lipase (RHC80267) activity suppresses CCL2-evoked Ca^{2+} signalling and transwell migration in monocytes. These effects were not due to a reduction in the number of cell surface CCR2 receptors. The effect of DAG kinase or DAG lipase inhibition could be mimicked by the addition of the DAG analogue 1-oleoyl-2-acetyl-glycerol (OAG) but was not rescued by application of exogenous phosphatidylinositol 4,5-bisphosphate. Suppressive effects of R59949, RHC80267 and OAG could be partially or fully reversed by the Gö6983 (pan PKC isoenzyme inhibitor) but not by Gö6976 (PKCα and PKCβ inhibitor). RNAi-mediated knock-down of DAG kinase α isoenzyme modulated CCL2-evoked Ca^{2+} responses in THP-1 cells.

Conclusions & Implications
Taken together, these data suggest that DAG production resulting from CCR2 activation is metabolised by both DAG kinase and DAG lipase pathways in monocytes, and that pharmacological inhibition of DAG catabolism or application suppresses signalling on the CCL2-CCR2 axis via a mechanism dependent upon a PKC isoenzymes(s) that are sensitive to Gö6983 but not Gö6976.

ABBREVIATIONS

CCL2, monocyte chemoattractant protein 1/chemokine ligand 2; DAG, diacylglycerol;
PBMCs, peripheral blood mononuclear cells; GADPH, glyceraldehyde 3-phosphate; AUC,
area under the curve

BACKGROUND

Chemokines are low molecular weight extracellular signalling peptides secreted by tissue either constitutively during homeostasis or *de novo* during an inflammatory response (Griffith et al., 2014). They are a diverse family of peptides (CC, CXC, CX_3C and XC chemokines) with a key role in the tissue recruitment and interstitial migration of leukocytes and other cell types, as well as acting both as chemoattractants and as cues for cellular arrest (Serbina & Pamer, 2006; Alon & Feigelson, 2012). The biological affects of chemokines are exerted through the activation of G protein-coupled receptors expressed on the cell surface of target cells. In addition to beneficial roles in homeostasis and immunity (Luther et al., 2002), the activity of chemokines is also associated with the onset and progression of chronic inflammatory diseases including atherosclerosis and rheumatoid arthritis (Zernecke & Weber, 2010). To this end, several drug discovery programmes have been initiated in an effort to pharmacologically intervene in chemokine receptor signalling for therapeutic benefit. Targeting single chemokine receptors has proven to be difficult to translating to clinical efficiency, likely due to a level of redundancy between chemokine receptor subtypes. Dual therapy has been proposed as a strategy to overcome this, in addition to targeting convergent second messenger pathways (Horuk et al., 2009).

The chemokine CCL2 (monocyte chemoattractant protein-1; MCP-1) activates CCR2, a G_i-coupled GPCR that elevates intracellular Ca^{2+} responses and inhibits adenylate cyclase activity (Campwala et al., 2014). Classical $CD14^+/CD16^-$ blood monocytes express high levels of cell surface CCR2 (Weber et al., 2000), in comparison to non-classical $CD14^+/CD16^+$ monocytes. In animal models of atherosclerosis it has been demonstrated that CCL2 signalling via CCR2 plays an important role in the size of monocyte/macrophage vascular wall infiltrate and size of atherosclerotic lesion (Boring et al., 1998; Gu et al., 1998; Veillard et al., 2005; Lutgens et al., 2005). CCL2 is also presented on the cell surface of vascular endothelium and participates in monocyte recruitment by stimulating firm adhesion and transmigration to the subendothelial space (Wang et al., 1995; Ashida et al., 2001; Maus et al., 2002). The importance of CCL2-CCR2 signalling does not match by our understanding of the signal transduction mechanisms that regulate functional responses in human monocytes (Cronshaw et al., 2006; Webb A et al., 2008).

Chemokines including CCL2 elictis intracellular Ca^{2+} responses in leukocytes and other cell types (Korniejewska et al., 2011; Campwala et al., 2014). The responses are pertussis toxin-sensitive and dependent upon phospholipase C (PLC) (Campwala et al., 2014). The involvement of PLC suggests that diacylglycerol (DAG) would be generated during generation of CCL2-evoked Ca^{2+} responses. DAG is a second messenger in it's own right and can modulate the activity of protein kinase C (PKC) and several ion channels. Once produced by cells DAG is radidly metabolised by two major pathways (1) conversion to phosphatidic acid by DAG kinase (Topham & Epand, 2009) and (2) hydrolysis to free fatty acid and monoacylglycerol by DAG lipase (Reisenberg et al., 2011). The aim of this study was to investigate the role of DAG metabolising enzymes on CCL2 evoked intracellular Ca^{2+} responses and cellular function in human monocytes.

MATERIALS & METHODS

Isolation of CD14+ monocyte from human peripheral blood

All work was undertaken with the approval of the Faculty of Medicine and Health Sciences Research Ethics Committee, University of East Anglia, and NHS Health Research Authority Ethics Committee. Healthy volunteer donor blood (National Health Service Blood and Transplant (Addenbrooke's Hospital, Cambridge University Hospital, UK) was used for the preparation of peripheral blood mononuclear cells (PBMCs) using methodology previously described (Layhadi et al., 2018). In brief, blood was layered on top of Histopaque-1077 (Sigma Aldrich) for centrifugation at 1000 x *g* for 25 mins. Buffy coat layers were collected and PBMCs were counted. CD14+ monocytes were positively selected from PBMC using anti-CD14+ magnetic beads (Miltenyi Biotech). Monocytes were resuspended in SBS buffer (mM): NaCl, 130; KCl, 5; $MgCl_2$, 1.2; $CaCl_2$, 1.5; D-glucose, 8; HEPES, 10; pH 7.4.

Culture of THP-1 human monocyte cells

THP-1 monocyte cells (CLS Cat# 300356/p804_THP-1, RRID:CVCL_0006) were cultured at 37ºC, 5% CO_2 in RPMI 1640 medium containing 2mM L-glutamine and supplemented with 10% (v/v) FBS, 50 IU/mL penicillin and 50 µg/mL streptomycin. Cells densities were maintained between 1 x 10^5 and 1 x 10^6 cells/mL.

Intracellular Ca²⁺ measurements

Experiments were conducted as described previously (Micklewright et al., 2018). Briefly, cells were treated with antagonists or vehicle controls for 30 minutes prior to challenge with agonists. Measurements were made using a 96-well plate reader with rapid well injection (Flexstation III, Molecular Devices). All experiments were performed in salt buffered solution (SBS) (pH 7.4), containing 130 mM sodium chloride, 5 mM potassium chloride, 1.2 mM magnesium chloride, 1.5 mM calcium chloride, 8 mM D-(+)-glucose and 10 mM HEPES. The cells were then loaded with 2 μM Fura-2AM (TEF Labs, Austin, TX, USA) in SBS supplemented with 0.01% (w/v) pluronic for 1 hour at 37 °C while being protected from light. The loading buffer was then removed and the cells were washed twice with SBS. Where applicable, the cells were incubated for a further 30 minutes with antagonists/vehicle or calcium-free SBS (SBS lacking 1.5 mM calcium chloride, but containing 2 mM EGTA, pH 7.4). All antagonists were dissolved in water or DMSO. Changes in intracellular Ca²⁺ concentration was measured as the ratio of emission at 510 nm following excitation at 340 and 380 nm (*F ratio*). Cells were treated with antagonists or vehicle controls for 30 minutes prior to challenge with agonists.

Flow cytometry

All sets were conducted at room temperature. 1×10^6 cells/mL were prepared in 100μL PBS for each marker and control experiment. Cell were treated for 30 minutes with drugs and vehicle controls prior to antibody labelled. Cells were incubated with 5µg/mL human BD Fc block (BD Pharmingen, New Jersey, USA) for 10 minutes. Next, (1:100) mouse monoclonal anti-CCR2 PE-conjugated antibody (BioLegend Cat# 357205, RRID:AB_2562058) or isotype control (Biolegend, USA) were added, and cells incubated in the dark for 30 minutes. Labelled cells were analysesd using a CytoFLEX flow cytometer (Beckman Coulter). Fluorescence intensity was read for PE using 496nm excitation and 578nm emission wavelengths, respectively. Living cells were gated according to their forward and side scatter profiles, and then histograms were plotted to compare fluorescence intensity for anti-CCR2 and isotype control antibodies using CytExpert Software (version 1.2.11, Beckman Coulter).

siRNA-mediated gene knockdown

THP-1 cells (2 x 10^5 final) were incubated overnight in complete RPMI (10% FBS) without antibiotics before cells were transfected using Dharmacon siRNA (25 nM final concentration) with DharmaFECT 2 transfection reagent (Dharmacon Research Inc, Cambridge, UK) using the manufacturer's protocol for a 96-well format. Scrambled siRNA and siRNA targeted against GADPH were used in negative and positive control experiments, respectively.

RNA extraction and non-quantitative RT-PCR

Total RNA was extracted from cells using Tri Reagent (Sigma Aldrich, Haverhill, UK) with subsequent DNase I treatment (Ambion). Complementary DNA was synthesised from 1 µg total RNA using Superscript II reverse transcriptase (Invitrogen, Waltham, USA). PCR was performed using a Taq polymerase readymix (Sigma Aldrich, Haverhill, UK) using the primers as given in **Table 1**.

Immunocytochemistry

THP-1 cells were seeded onto poly L-lysine coated coverslips followed by fixation with 4%(w/v) paraformaldehyde for 15 mins at room temperature, and permeabilization with 0.25%(v/v) Triton X-100 for 10 minutes. Fixed and permeabilised cells were blocked with 1% (w/v) bovine serum albumin. Cells were incubated with primary antibodies overnight at 4ºC, followed by washing and incubation with Alexa Fluor 488-conjugated secondary antibodies. In negative control experiments, primary antibodies were omitted. Rabbit polyclonal primary antibodies (anti-DGKδ, Sigma HPA049101, RRID:AB_2680630; anti-DGKγ, Abcam ab151967, RRID:AB_151967; anti-DGKη, Abcam ab80693, RRID:AB_1658681; anti DGKζ, Abcam ab111047, RRID:AB_10858121; anti-DAGLα Abcam ab106979, RRID:AB_10862875; anti-DAGLβ) were used in conjunction with a goat anti-rabbit secondary antibody (Thermo Fisher Scientific Cat# A27034, RRID:AB_2536097). Mouse monoclonal primary antibodies (anti-PKCα, Santa Cruz Biotechnology sc-8393, RRID:AB_628142; anti-DGKα, Santa Cruz Biotechnology sc-271644, RRID:AB_10708574; anti-DGKε, Santa Cruz Biotechnology Cat# sc-100372, RRID:AB_2245858; anti-DGKθ, Santa Cruz Biotechnology sc-137197, RRID:AB_2292802) were used in conjunction with goat

anti-mouse seceondary antibody ((Thermo Fisher Scientific Cat# A28175, RRID:AB_2536161). Fluorescent and brightfield images were captured using a Zeiss AxioPlan 2ie epifluorescent microscope.

Transmigration assays

Transwell migration assays were performed as previously described (Micklewright et al., 2018). Briefly, assays were performed in 24-well plates using polyethylene terephthalate membrane inserts with 3µm pores. 1 x 10^6 cells in RPMI (no serum) with vehicle or drug treatment were added to the lower chamber. Assays were performed for 2 hours at 37°C, and the cells that had migrated were on the underside of the transwell insert membrane using crystal violet staining. Chemotactic index was calculated as the ratio of cells that migrated towards CCL2 over vehicle control. These experiments were blinded.

DAG assay

DAG levels were measured using an enzyme-linked fluorescence assay (Cell Biolabs). Accumulation of fluorescence product has measured using 530 nm exicitation and 590 nm emission. $5x10^7$ THP-1 cells in suspension were incubated at 20°C in SBS solution for 2 hours prior to CCL2 challenge. Cells were exposed to inhibitors for 30 mins before challenge with CCL2 or vehicle. Following cell exposure to CCL2 for 1 or 2 mins, cells were plunged on ice and sonicated in methanol, proceeded by extraction of organic phase in chloroform. Total protein was measured by Bradford assay and used to normalise fluorescence measurements.

Cell Toxicity Assay

Potential cytotoxic effects of drug treatments were measured by quantification of lactate dehydrogenase (LDH) release from cells using colorimetric assay (Abcam) as for Campwala et al (2014). To mimic experimental conditions, $1x10^6$ THP-1 or freshly isolated monocytes were incubated with test compounds in SBS assay buffer for 30 minutes prior to conducting the LDH assay. 0.1% triton X-100 was used in positive control experiments. These experiments were blinded.

Data analysis & statistics

The data and statistical analysis comply with the recommendations on experimental design and analysis in pharmacology (Curtis et al., 2015). Data analysis was performed using Origin Pro 9.0 software (Origin Lab, USA). Dose-response curves were fitted assuming a Hill coefficient of 1, with the Hill equation used to determine the degree of cooperation. Figure data points represent mean values $\pm$ SEM (error bars). N is defined as number of technical repeats or biological repeats (donor number) for experiments with THP-1 cells and freshy isolated CD14$^+$ monocytes, respectively. Statistical significance was determined using Student's paired t-test for two sample and ANOVA for multiple sample datasets. A confidence interval of 5% (P<0.05) is applied throughout.

Blinding in experiments

Experimental manipulations were blinded to the experimentor were technically feasible.

Chemicals and reagents

Unless otherwise stated, all chemicals and reagents were purchased from Sigma-Aldrich (Haverhill, UK).

Nomenclature of targets and ligands

Key protein targets in this article are hyperlinked to corresponding enteries in http://www.guidetopharmacology.org the common portal for data from IUPHAR/BPS Guide to Pharmacology (Harding et al., 2018), and are permanently archived in the Concise Guide to PHARMACOLOGY 2017/2018 (Alexander et al., 2017a,b).

RESULTS

DAG kinase and DAG lipase inhibitors attenuate CCL2-evoked intracellular Ca^{2+} signals and migration in freshly isolated human monocytes and THP-1 monocytic cells

CCL2 evoked concentration-dependent intracellular Ca^{2+} responses in freshly isolated human CD14$^+$ monocytes (**Figure 1A)** with an EC_{50} of 33 ± 4nM (N=8) (**Figure 1B**). These responses were abolished by the CCR2 selective antagonist BMSCCR222 (**Figure 1C**; IC_{50} 9.2 ± 1.2 nM, N=8). CCL2 also evoked Ca^{2+} responses in THP-1 monocytes (**Figure 1D**) with an EC_{50} 45 ± 12nM (N=6) (**Figure 1E**), and these response were abolished by BMSCCR222 (**Figure 1F**; IC_{50} 8.4 ± 1.4nM, N=6). These data demonstrate that CCL2 evoked intracellular Ca^{2+} responses are dependent upon CCR2 activation in both freshly isolated monocytes and the THP-1 monocytic cells. CCL2-evoked intracellular Ca^{2+} responses in freshly isolated monocytes (**Figure 1A**) and THP-1 monocytic cells (**Figure 1D**) was abolished following phospholipase C inhibition with U73122.

CCR2 is a G_i-coupled GPCR that elicits intracellular Ca^{2+} responses in a pertussis toxin-sensitive and phospholipase C-dependent fashion (Campwala et al., 2014). This signal transduction mechanism generates diacylglycerol (DAG), and we therefore investigated the impact of DAG metabolism on CCL2 evoked Ca^{2+} responses. In THP-1 monocytes, R59949 (a small molecule inhibitor of DAG kinase; de Chaffroy de Courcelles et al., 1989) attenuated CCL2-evoked Ca^{2+} signalling (**Figure 2A**) with a half-maximal concentration of 8.6 ± 1.2µM (N=7) (**Figure 2B**). Maximal response in THP-1 cells were inhibited by approximately 70% using 30µM R59949 (**Figure 2C**). Similarly, CCL2-evoked Ca^{2+} responses were suppressed by RHC80267 (**Figure 2D**), an inhibitor of DAG lipase (Dale & Penfield, 1987). RHC80267 inhibited the response with a half-maximal concentration of 9.3 ± 1.0 µM (N=7) (**Figure 2E**), reducing the maximal response to CCL2 by approximately 30% using 30µM RHC80267 (**Figure 2F**). In addition to CCL2-evoked Ca^{2+} signals, both DAG kinase or DAG lipase inhibition attenuated CCL2 mediate THP-1 chemotaxis (**Figure 2G**). Application of CCL2 to THP-1 monocytic cells caused a rapid increase in cellular DAG (**Figure 2H**). As for CCL2 evoked Ca^{2+} signals (**Figure 1D**), phospholipase C inhibition with U73122 the CCL-2 evoked increase in cellular DAG (**Figure 2H**). Both R59949 and RHC80267 significantly enhanced CCL2-evoked DAG elevation (**Figure 2H**), consistent with a role of DAG kinase and DAG lipase in metabolising DAG following receptor-mediated synthesis.

Importantly, DAG kinase and DAG lipase inhibition attenuated CCL2-evoked signalling in freshly isolated human CD14$^+$ monocytes (**Figure 3**). R59949 (30µM; **Figure 3A**) and RHC80267 (30µM; **Figure 3B**) inhibited CCL2-evoked Ca^{2+} signals, inhibiting the peak Ca^{2+}

response by approximately 75% and 30% (**Figure 3C**); respectively. Furthermore, both DAG kinase and DAG lipase inhibited CCL2 stimulated migration in freshly isolated monocytes (**Figure 3D**). Interestingly, intracellular Ca^{2+} responses elicited as a consequence of formyl peptide receptor with *N*-formylmethionine-leucyl-phenylalanine (fMLP) activation on monocytes were insensitive to either R59949 (**Figure 3E**) or RHC80267 (**Figure 3F**), which suggests that DAG kinase or DAG lipase inhibition is not a generic regulator of receptor-mediated Ca^{2+} signalling in monocytes (**Figure 3G**). Though the focus of this study is CCL2, we also investigate the effect of R59949 and RHC80267 on CCL5-mediated responses in freshly isolated monocytes. CCL5 has been reported to activate CCR1, CCR3 and CCR5 receptors (de Wit et al., 2016) and is also implication with the onset and progression of atherosclerosis (Schober et al., 2002). In monocytes, we observed that CCL5 mediates intracellular Ca^{2+} response through activation of CCR1, but not CCR3 or CCR5 (**Supplemental Figure 1**). The activity of CCR1 is also attenuated following following DAG kinase or DAG lipase inhibition. However, the ability of CXCL1, which is implicated in monocyte mobilization under chronic inflammatory conditions (Drechsler et al., 2015), to evoked intracellular Ca^{2+} responses in monocytes was attenuated by inhibition of DAG kinase but not DAG lipase (**Supplemental Figure 2**). In monocytes, we observe that CXCL1-evoked Ca^{2+} responses are mediated by CXCR2 activation (**Supplemental Figure 2**).

Next we profiled the expression of DAG kinase and DAG lipase isoforms expressed in freshly isolated human CD14$^+$ monocytes and THP-1 monocytic cells. RT-PCR analysis of mRNA transcripts revealed an overlapping expression profile of DAG kinase and DAG lipase isoforms in CD14$^+$ monocytes and THP-1 cells (**Table 1**). For DAG kinase isoforms, α, γ, δ, η, ε, θ, κ and ζ were expressed by both cell types, and β and ι were not. For DAG lipase isoforms, isoforms α and β were expressed by CD14$^+$ monocytes and THP-1 cells (**Table 1**). To corroborate these findings, we confirmed expression at the protein level by immunocytochemistry in THP-1 cells (**Supplemental Figure 3**).

The amount of cell surface CCR2 is unaffected by DAG kinase or DAG lipase inhibition

A possible mechanism underlying the reduced responsivity to CCL2 following inhibition of DAG metabolism is a reduction in the number of cell surface CCR2 receptors. To test this hypothesis we quantified CCR2 cell surface expression in freshly isolated monocytes and THP-

1 cells following R59949 or RHC80267 treatment by flow cytometry. A PE-conjugated antibody recognising human CCR2 labelled CCR2 CD14$^+$ monocytes (**Figure 4A**) and THP-1 cells (**Figure 4B**) over an isotype control. R59949 and RHC80267 were applied to cells to mimic the protocol used to investigating Ca^{2+} signalling. Despite this, neither R59949 or RHC80267 had any significant effect on CCR2 cell surface expression in THP-1 cells or human CD14$^+$ monocytes (**Figure 4**).

To further understand the role of DAG kinase and DAG lipase activity in shaping CCL2-evoked intracellular Ca^{2+} responses, we examined the effect of the inhibitors on the responses in the absence of extracellular Ca^{2+} to negate Ca^{2+} entry. Under these conditions CCL2 evoked a rapidly rising but transient Ca^{2+} response which returned to baseline (**Figure 5A**). DAG kinase inhibition with R5549 attenuated the peak response but lead to a sustained plateau phase after the transient response (**Figures 5A & 5B**), exemplified by an increased area under the curve (AUC) (**Figure 5C**). Unlike DAG kinase inhibition, DAG lipase inhibition with RHC80267 did not effect the transient phase (**Figures 5D & 5E**) but did lead to a sustained plateau phase after the transient response (**Figure 5F**). The AUC for CCL2 evoked responses under conditions of no external Ca^{2+} was significantly large following DAG lipase inhibition compared to DAG kinase inhibition, reflecting the difference in degree of inhibition observed in conditions with external Ca^{2+} (**Figure 2**). These data suggest though DAG kinase and DAG lipase inhibition both suppress the global Ca^{2+} response to CCL2, they may do so via different mechanisms.

Attenuative effect of DAG metabolism inhibitors is mimicked by 1-oleoyl-2-acetyl-glycerol but not rescued by phosphatidylinositol 4,5-bisphosphate

Following receptor-mediated hydrolysis of PIP$_2$ to DAG and IP$_3$, DAG is used as a substrate for the rapid resynthesis of PIP$_2$. We therefore reasoned that limiting DAG metabolism could therefore limit PIP$_2$ resynthesis and reduce the pool of PIP$_2$ available for receptor-mediated hydrolysis, this in time could underlie the attenuated CCL2-mediated Ca^{2+} response observed. To this end, to rescue the effect of DAG kinase inhibition by supplementing with exogenous PIP$_2$ (Kantonen et al., 2011). However, in these experiments exogenous PIP$_2$ did not limit the ability of R59949 to suppress CCL2-evoked Ca^{2+} signals (**Figures 6A & 6B**), suggesting PIP$_2$ availability did not underlie the inhibition. We therefore attempted to address whether the accumulation of DAG itself following pharmacological inhibition of its metabolism could

mediate the attenuation of Ca^{2+} signalling. We observed that 1-oleoyl-2-acetyl-sn-glycerol (OAG), a membrane permeable DAG analogue (Assani et al., 2017), could mimic the effect of DAG kinase or DAG lipase inhibition (**Figure 6C**) and inhibit CCL2-evoked Ca^{2+} signalling in a concentration fashion (**Figure 6D**). The half-maximal concentration for OAG was 9.2 ± 1.2 μM (N=6) and the maximum CCL2 response was suppressed by approximately 70% at 30μM OAG (**Figure 6E**).

Differential dependency on PKC for effects of DAG metabolism inhibitors and 1-oleoyl-2-acetyl-glycerol

As DAG is a well characterised activator of protein kinase C (PKC), we sought to test whether PKC activity was required for the suppressive action of OAG, DAG kinase and DAG lipase inhibition. RT-PCR analysis of PKC isoform mRNA transcripts revealed expression of α, β, δ, η, ε, θ, ι and ζ but not γ in THP-1 cells (**Table 1**). We confirmed the expression of PKCα by immunocytochemistry (**Supplemental Figure 3**). The expression pattern was the same in freshly isolated CD14$^+$ monocytes except that PKCε was not expressed (**Table 1**). Due to the diverse repertoire of PKC isoforms expressed, we employed pharmacological tools that allowed discrimination between classical DAG and Ca^{2+}-dependent isoforms (α, β and γ; blocked by Gö6976) and DAG dependent but Ca^{2+}-independent isoforms (δ, ε, η or θ; blocked by Gö6983); Gö6983 also blocks α, β and γ isoforms (Gschwendt et al., 1998; Goekjian et al., 1999). 100nM Gö6983 (Young et al., 2014) had no effect on the control Ca^{2+} response to CCL2 (**Figure 7A**), however 100nM Gö6976 (Lin et al., 2011) significantly inhibited the response (**Figure 7A**). Gö6983 could rescue the response inhibited by OAG (**Figure 7B**), R59949 (**Figure 7C**) or RHC80267 (**Figure 7D**), though Gö6976 could not (**Figure 7B-D**). These data, summarised in **Figure 7E,** suggest that the inhibitory action of exogenous DAG (OAG) on DAG metabolism is mediated via a Ca^{2+}-independent PKC isoform. The inhibitory action of R59949 and RHC80267 on CCL2-evoked Ca^{2+} in freshly isolated monocytes could also be reversed by Gö6983 (N=5; **Figure 7F**).

The Ca^{2+}-sensitive isoform PKCα regulates CCL2-evoked Ca^{2+} signalling in THP-1 cells

A striking observation of the experiments with Gö6976 was its ability to inhibit CCL2-evoked Ca^{2+} signalling without pharmacological manipulation of DAG metabolism. These data

suggest a DAG and Ca^{2+}-dependent PKC isoform may regulate the CCL2 response, and to investigate this further we attempted siRNA-mediated knockdown studies of the classical Ca^{2+}-sensitive PKC isoform PKCα. In this experiments, siRNA delivery to THP-1 monocytes could inhibit CCL2-evoked Ca^{2+} responses versus scrambled siRNA counterparts (**Figure 8A**). Though the response peak was unaffected (**Figure 8B**), PKCα knockdown significantly reduced response AUC (**Figure 8C**). Quantitative RT-PCR confirmed PKCα mRNA knockdown of approximately 50% versus scrambled siRNA counterparts (**Figure 8D**). These data suggest the activity of PKCα is required for THP-1 cells to respond to CCL2 at control levels.

LDH release assays were performed to test for potential cytotoxic effects of inhibitor treatments applied throughout the study (**Supplemental Figure 4**).

DISCUSSION

This study reconfirms that CCR2 is the cognate receptor for CCL2 in human CD14^{+} monocytes and THP-1 cells. We also provide molecular and function evidence that both DAG kinase and DAG lipase are functional routes for the metabolism of DAG arising from receptor-mediated DAG production. These results corroborate studies in T-lymphocytes (Lee et al., 2012) and cancer cells (Rainero et al., 2014) that demonstrate a role for DAG kinases in modulating chemokine functionality. Our data also reveal CCL5 signalling via CCR1 is reglated by both DAG kinase and DAG lipase activity, though lack of effect of DAG lipase inhibition on CXCL1-CXCR2 signalling is suggestive that this mechanism cannot be generalised for all chemokine action at monocytes.

The data suggests that inhibitors of both of DAG kinase and DAG lipase are effective in reducing the efficacy of CCL2 signalling in monocytes, as the response maxima is significantly attenuated with little change in CCL2 EC_{50} values. As the effects of DAG kinase and DAG lipase inhibition are mimicked by OAG and not rescued by addition of exogenous PIP_2, the effect on CCL2 signalling of inhibiting DAG metabolism is likely to be due to the accumulation of DAG rather than limitation of a DAG metabolite or PIP_2 synthesis. If this is the case, the data suggests that there is no redundancy between kinase or lipase-dependent metabolic pathways for DAG in human monocytes, and processes that modulate the activity of these

enzymes have the potential to modulate CCL2 signalling efficacy. Although CCR2 receptors are classical GPCRs and can undergo internalisation as part of mechanisms of receptor desensitisation (Dzenko et al., 2001; Volpe et al., 2012), the data presented here suggests the mechanism via which inhibition of DAG metabolism causes loss of CCL2 signalling efficacy is not via a reduction in the cell surface population of CCR2 receptors. This therefore suggests that the inhibitory mechanism must involve modulation of the CCR2 receptor itself, an auxillary subunit or a downstream effector protein. As the effects of OAG, DAG kinase inhibition and DAG lipase inhibition are reversed by the broadspectrum PKC inhibitor Gö6983 but not Gö6976, a selective inhibitor of Ca^{2+}-dependent PKC isoforms, this is suggests that the inhibitor effects of DAG accumulation are mediated by a Ca^{2+}-independent PKC isoform. Analysis of PKC isoform expression suggests that PKCδ, PKCε, PKCη, PKCθ and PKCζ are potential effectors of the inhibitory actions of DAG in monocytes. Previous studies in monocytes have documented translocation of both Ca^{2+}-dependent and Ca^{2+}-independent PKC isoform from the cytoplasm to the plasma membrane upon stimulation with CCL2 (Zhang et al., 2003). However opioid receptor activation, which inhibits CCL2 signalling via heterologous desensitisation, causes membrane recruitment of only Ca^{2+}-independent PKC isoforms (Zhang et al., 2003). Such studies support a role for Ca^{2+}-independent PKC isoforms as negative regulators of CCR2 receptor activity. The target of PKC is unlikely to be the CCR2 receptor itself as consensus sequences for PKC-dependent phosphorylation are absent from the cytoplasmic sections of the receptors, although other chemokine receptor, such as CXCR4, are phosphorylated directly by PKC (Luo et al., 2017).

The intracellular Ca^{2+} signal generated following CCR2 activation in monocytes most likely involves direct release of Ca^{2+} from ER stores but also Ca^{2+} through plasma membrane channels (Nardelli et al., 1999). Experiments in the absence of extracellular Ca^{2+} support this as CCL2 can still elicit a response though transient and lacking a substantial plateau phase. The shape of the intracellular Ca^{2+} response is also differentially modulated by DAG kinase and DAG lipase inhibitors when the possibility of Ca^{2+} influx is negated. Both R59949 and RHC80267 elevate the plateau phase of release, but only R59949 inhibits the peak Ca^{2+} response in the absence of extracellular Ca^{2+}. This suggests that there may be some discrimination regarding how DAG elevation, directly or indirectly, regulates the ability of CCR2 to release stored Ca^{2+} (Bartlett et al., 2015). Monocytes express a large repertoire of DAG kinase isoforms and as R59949 is a pan DAG kinase inhibitor we cannot determine

whether redundancy exists between isoforms or whether only some subtypes participate in the regulation of CCR2 activity. siRNA-mediated knockdown studies reveal DAG kinase α as a candidate, at least in THP-1 cells. DAG kinase α has been implicated previously in immune cell function (Sanjuan et al., 2003).

In summary, we demonstrate that inhibition of DAG kinases and DAG lipases are a novel pharmacological route to suppress CCL2-mediated intracellular Ca^{2+} signalling and migration in human monocytes. We suggest the underlying mechanism involves DAG accumulation and activation of Ca^{2+}-independent PKC isoforms.

REFERENCES

Alon R, & Feigelson SW (2012). Chemokine-triggered leukocyte arrest: force-regulated bi-directional integrin activation in quantal adhesive contacts. Curr Opin Cell Biol 24: 670-676.

Ashida N, Arai H, Yamasaki M, & Kita T (2001). Distinct signaling pathways for MCP-1-dependent integrin activation and chemotaxis. J Biol Chem 276: 16555-16560.

Assani K, Shrestha CL, Robledo-Avila F, Rajaram, MV, Partida-Sanchez, S, Schlesinger, LS et al (2017). Human Cystic Fibrosis Macrophages Have Defective Calcium-Dependent Protein Kinase C Activation of the NADPH Oxidase, an Effect Augmented by *Burkholderia cenocepacia*. J Immunol 198: 1985-1994.

Bartlett PJ, Metzger W, Gaspers LD, & Thomas AP (2015). Differential Regulation of Multiple Steps in Inositol 1,4,5-Trisphosphate Signaling by Protein Kinase C Shapes Hormone-stimulated Ca2+ Oscillations. J Biol Chem 290: 18519-18533.

Boring L, Gosling J, Cleary M, & Charo IF (1998). Decreased lesion formation in CCR2-/- mice reveals a role for chemokines in the initiation of atherosclerosis. Nature 394: 894-897.

Campwala H, Sexton DW, Crossman DC, & Fountain SJ (2014). P2Y(6) receptor inhibition perturbs CCL2-evoked signalling in human monocytic and peripheral blood mononuclear cells. J Cell Sci 127: 4964-4973.

Cronshaw DG, Owen C, Brown Z, & Ward SG (2004). Activation of phosphoinositide 3-kinases by the CCR4 ligand macrophage-derived chemokine is a dispensable signal for T lymphocyte chemotaxis. J Immunol 172: 7761-7770.

Curtis MJ, Bond RA, Spina D, Ahluwalia A, Alexander SP, Giembycz MA, et al. (2015). Experimental design and analysis and their reporting: new guidance for publication in BJP. Br J Pharmacol 172: 3461-3471.

Dale MM, & Penfield A (1987). Comparison of the effects of indomethacin, RHC80267 and R59022 on superoxide production by 1,oleoyl-2,acetyl glycerol and A23187 in human neutrophils. Br J Pharmacol 92: 63-68.

de Chaffoy de Courcelles D, Roevens P, Van Belle H, Kennis L, Somers Y, & De Clerck F (1989). The role of endogenously formed diacylglycerol in the propagation and termination of platelet activation. A biochemical and functional analysis using the novel diacylglycerol kinase inhibitor, R 59 949. J Biol Chem 264: 3274-3285.

Drechsler M, Duchene J & Soehnlein O (2015). Chemokines control mobilization, recruitment, and fate of monocytes in atherosclerosis. Arterioscler Thromb Vasc Biol 35: 1050-5.

De Wit RH, de Munnik SM, Leurs R, Wischer HF & Smit MJ (2016). Molecular Pharmacology of Chemokine Receptors. Methods Enzymol 570: 457 – 515.

Dzenko KA, Andjelkovic AV, Kuziel WA, & Pachter JS (2001). The chemokine receptor CCR2 mediates the binding and internalization of monocyte chemoattractant protein-1 along brain microvessels. J Neurosci 21: 9214-9223.

Goekjian PG, & Jirousek MR (1999). Protein kinase C in the treatment of disease: signal transduction pathways, inhibitors, and agents in development. Curr Med Chem 6: 877-903.

Griffith JW, Sokol CL, & Luster AD (2014). Chemokines and chemokine receptors: positioning cells for host defense and immunity. Annu Rev Immunol 32: 659-702.

Gschwendt M, Dieterich S, Rennecke J, Kittstein W, Mueller HJ, & Johannes FJ (1996). Inhibition of protein kinase C mu by various inhibitors. Differentiation from protein kinase c isoenzymes. FEBS Lett 392: 77-80.

Gu L, Okada Y, Clinton SK, Gerard C, Sukhova GK, Libby P, et al. (1998). Absence of monocyte chemoattractant protein-1 reduces atherosclerosis in low density lipoprotein receptor-deficient mice. Mol Cell 2: 275-281.

Harding SD, Sharman JL, Faccenda E, Southan C, Pawson AJ, Ireland S, et al. (2018). The IUPHAR/BPS Guide to PHARMACOLOGY in 2018: updates and expansion to encompass the new guide to IMMUNOPHARMACOLOGY. Nucleic Acids Res 46: D1091-D1106.

Horuk R (2009). Chemokine receptor antagonists: overcoming developmental hurdles. Nat Rev Drug Discov 8: 23-33.

Kantonen S, Hatton N, Mahankali M, Henkels, KM, Park, H, Cox, D et al., (2011). A novel phospholipase D2-Grb2-WASp heterotrimer regulates leukocyte phagocytosis in a two-step mechanism. Mol Cell Biol 31: 4524-37.

Korniejewska A, McKnight AJ, Johnson Z, Watson ML, & Ward SG (2011). Expression and agonist responsiveness of CXCR3 variants in human T lymphocytes. Immunology 132: 503-515.

Layhadi JA, Turner J, Crossman D, & Fountain SJ (2018). ATP Evokes Ca(2+) Responses and CXCL5 Secretion via P2X4 Receptor Activation in Human Monocyte-Derived Macrophages. J Immunol 200: 1159-1168.

Lee D, Kim J, Beste, MT, Korestzky, GA & Hammer GL (2012). Diacylglycerol kinase zeta negatively regulates CXCR4-stimulated T lymphocyte firm arrest to ICAM-1 under shear flow. Integr Biol 4: 606-614

Lin YF, Leu SJ, Huang HM & Tsai YH (2011). Selective activation of specific PKC isoforms dictating the fate of CD14(+) monocytes towards differentiation or apoptosis. J Cell Physiol 226: 122-31.

Luo J, Busillo JM, Stumm R, & Benovic JL (2017). G Protein-Coupled Receptor Kinase 3 and Protein Kinase C Phosphorylate the Distal C-Terminal Tail of the Chemokine Receptor CXCR4 and Mediate Recruitment of beta-Arrestin. Mol Pharmacol 91: 554-566.

Lutgens E, Faber B, Schapira K, Evelo CT, van Haaften R, Heeneman S, et al. (2005). Gene profiling in atherosclerosis reveals a key role for small inducible cytokines: validation using a novel monocyte chemoattractant protein monoclonal antibody. Circulation 111: 3443-3452.

Luther SA, Bidgol A, Hargreaves DC, Schmidt A, Xu Y, Paniyadi J, et al. (2002). Differing activities of homeostatic chemokines CCL19, CCL21, and CXCL12 in lymphocyte and dendritic cell recruitment and lymphoid neogenesis. J Immunol 169: 424-433.

Maus U, Henning S, Wenschuh H, Mayer K, Seeger W, & Lohmeyer J (2002). Role of endothelial MCP-1 in monocyte adhesion to inflamed human endothelium under physiological flow. Am J Physiol Heart Circ Physiol 283: H2584-2591.

Micklewright JJ, Layhadi JA, & Fountain SJ (2018). P2Y12 receptor modulation of ADP-evoked intracellular Ca(2+) signalling in THP-1 human monocytic cells. Br J Pharmacol 175: 2483-2491.

Nardelli B, Tiffany HL, Bong GW, Yourey PA, Morahan DK, Li Y, et al. (1999). Characterization of the signal transduction pathway activated in human monocytes and dendritic cells by MPIF-1, a specific ligand for CC chemokine receptor 1. J Immunol 162: 435-444.

Rainero E, Cianflone C, Porporato PE, Chianale F, Malacame V, Bettio V et al. (2014). The diacylglycerol kinase α/atypical PKC/β1 integrin pathway in SDF-1α mammary carcinomainvasiveness. PLoS ONE 9:e97144.

Reisenberg M, Singh PK, Williams G, & Doherty P (2012). The diacylglycerol lipases: structure, regulation and roles in and beyond endocannabinoid signalling. Philos Trans R Soc Lond B Biol Sci 367: 3264-3275.

Sanjuan MA, Pradet-Balade B, Jones DR, Martinez AC, Stone JC, Garcia-Sanz JA, et al. (2003). T cell activation in vivo targets diacylglycerol kinase alpha to the membrane: a novel mechanism for Ras attenuation. J Immunol 170: 2877-2883.

Schober A, Manka D, von Hundleshausen P, Huo Y, Hanrath P, Saremock IJ, et al. (2002). Deposition of platelet RANTES triggering monocyte recruitment requires P-selectin and is involved in neointima formation after artery injury. Circulation 106: 1523-9.

Serbina NV, & Pamer EG (2006). Monocyte emigration from bone marrow during bacterial infection requires signals mediated by chemokine receptor CCR2. Nat Immunol 7: 311-317.

Topham MK, & Epand RM (2009). Mammalian diacylglycerol kinases: molecular interactions and biological functions of selected isoforms. Biochim Biophys Acta 1790: 416-424.

Veillard NR, Steffens S, Pelli G, Lu B, Kwak BR, Gerard C, et al. (2005). Differential influence of chemokine receptors CCR2 and CXCR3 in development of atherosclerosis in vivo. Circulation 112: 870-878.

Volpe S, Cameroni E, Moepps B, Thelen S, Apuzzo T, & Thelen M (2012). CCR2 acts as scavenger for CCL2 during monocyte chemotaxis. PLoS One 7: e37208.

Wang DL, Wung BS, Shyy YJ, Lin CF, Chao YJ, Usami S, et al. (1995). Mechanical strain induces monocyte chemotactic protein-1 gene expression in endothelial cells. Effects of mechanical strain on monocyte adhesion to endothelial cells. Circ Res 77: 294-302.

Webb A, Johnson A, Fortunato M, Platt A, Crabbe T, Christie MI, et al. (2008). Evidence for PI-3K-dependent migration of Th17-polarized cells in response to CCR2 and CCR6 agonists. J Leukoc Biol 84: 1202-1212.

Weber C, Belge KU, von Hundelshausen P, Draude G, Steppich B, Mack M, et al. (2000). Differential chemokine receptor expression and function in human monocyte subpopulations. J Leukoc Biol 67: 699-704.

Young SH, Rey O, Sinnett-Smith J & Rozengurt, E (2014). Intracellular Ca2+ oscillations generated via the Ca2+-sensing receptor are mediated by negative feedback by PKCα at Thr888. Am J Physiol Cell Physiol 306: C298-306.

Zernecke A, & Weber C (2010). Chemokines in the vascular inflammatory response of atherosclerosis. Cardiovasc Res 86: 192-201.

Zhang N, Hodge D, Rogers TJ, & Oppenheim JJ (2003). Ca2+-independent protein kinase Cs mediate heterologous desensitization of leukocyte chemokine receptors by opioid receptors. J Biol Chem 278: 12729-12736.
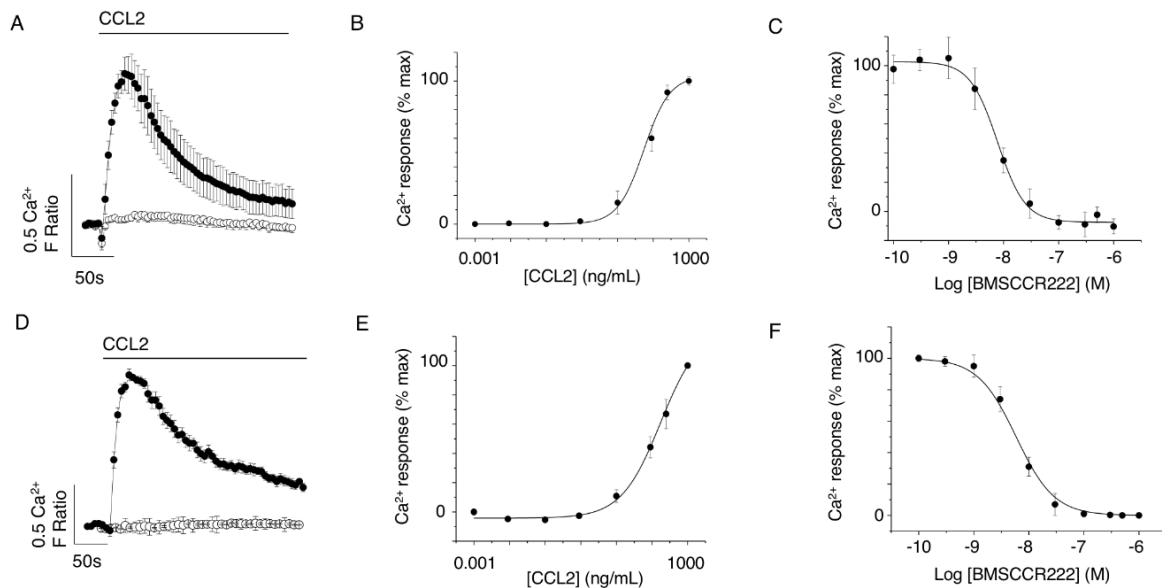
Figure 1 CCR2 is the cognate receptor for CCL2 in freshly isolated human monocytes and THP-1 monocytic cells. (A) Averaged (N=8) intracellular Ca^{2+} response to CCL2 (50 ng/mL) in freshly isolated $CD14^+$ human monocytes. Response in the presence (*open circles*) and absence *(closed circles)* of 5μM U73122 ($N=6$; $P<0.05$). (B) Concentration-response curve for CCL2-evoked responses in freshly isolated monocytes (N=8; $EC_{50} = 33\pm4nM$). (C) Concentration-inhibition curve for selective CCR2 receptor antagonist BMSCCR222 ($IC_{50} = 9\pm1nM$; N=8) against Ca^{2+} responses evoked by CCL2 (50 ng/mL) in freshly isolated monocytes. (D) Averaged (N=6) intracellular Ca^{2+} response to CCL2 (50 ng/mL) in THP-1 cells. Response in the presence (*open circles*) and absence *(closed circles)* of 5μM U73122 ($N=6$; $P<0.05$). (E) Concentration-response curve for CCL2-evoked responses in THP-1 cells (N=6; $EC_{50} = 45\pm12nM$). (F) Concentration-inhibition curve for BMSCCR222 ($IC_{50} = 8\pm1nM$; N=6) against Ca^{2+} responses evoked by CCL2 (50 ng/mL) in THP-1 cells. Responses are in the presence of vehicle alone (*closed circles*) or in the presence of U73122 (*open circles*). F ratio is the Ca^{2+} response as measured by the Fura-2 emission intensity ratio when excited at 340 and 380 nm. Data in concentration-response/inhibition curves is expressed as a percentage of the control response in the presence of vehicle alone.
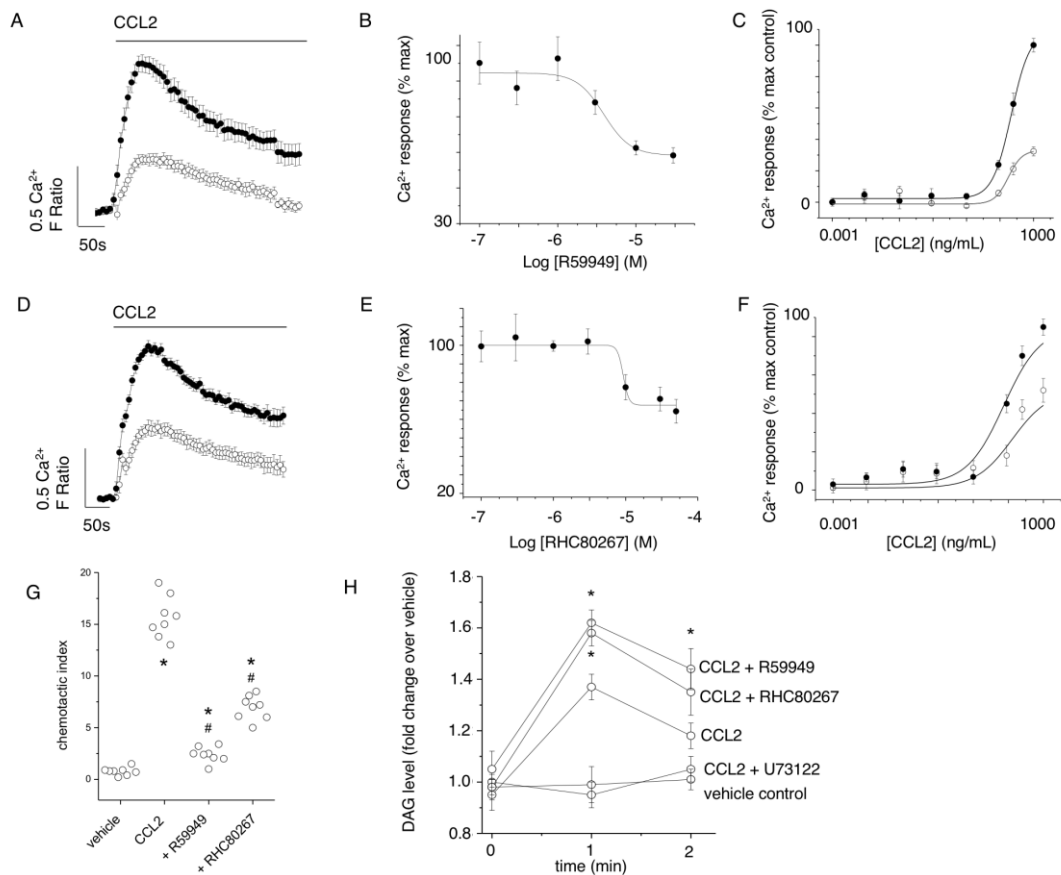
Figure 2 Inhibitors of DAG kinase and DAG lipase attenuate CCL2-evoked Ca^{2+} signalling and migration in THP-1 cells. (A) Effect of DAG kinase inhibitor R59949 (30μM) on Ca^{2+} responses evoked by CCL2 (50 ng/mL) (*N*=7). Averaged responses are shown in the presence of vehicle (*closed circles*) and inhibitor (*open circles*). (B) R59949 concentration-inhibition curve (IC$_{50}$ = 9±1μM; *N*=7) against Ca^{2+} responses evoked by CCL2 (50 ng/mL). (C) Effect of 30μM R59949 on CCL2 concentration-response curve (*N*=7). (D) Effect of DAG lipase inhibitor RHC80267 (30μM) on Ca^{2+} responses evoked by CCL2 (50 ng/mL) (*N*=7). Averaged responses are shown in the presence of vehicle (*closed circles*) and inhibitor (*open circles*). (E) RHC80267 concentration-inhibition curve (IC$_{50}$ = 9±1μM; *N*=7) against Ca^{2+} responses evoked by CCL2 (50 ng/mL). (F) Effect of 30μM RHC80267 on CCL2 concentration-response curve (*N*=7). (G) Effect of R59949 (30μM) and RHC80267 (30μM) on THP-1 transmigration to CCL2 (3 ng/mL). * denotes *P*<0.05 versus vehicle and # denotes *P*<0.05 versus CCL2 alone (*N*=8). F ratio is the Ca^{2+} response as measured by the Fura-2 emission intensity ratio when excited at 340 and 380 nm. Data in concentration-response/inhibition curves is expressed as a percentage of the control response in the presence of vehicle alone. (H) Biochemical measurement of DAG changes in THP-1 cells. Cells preincubated for 30 minutes with either U73122 (5μM), R59949 (30μM) or RHC80267 (30μM) prior to CCL2 challenge (50ng/mL) for 1 or 2 mins (*N*=6). *Vehicle control*; cells are are preincubated with vehicle and not challenged with CCL2. * denotes *P*<0.05 versus CCL2 alone.
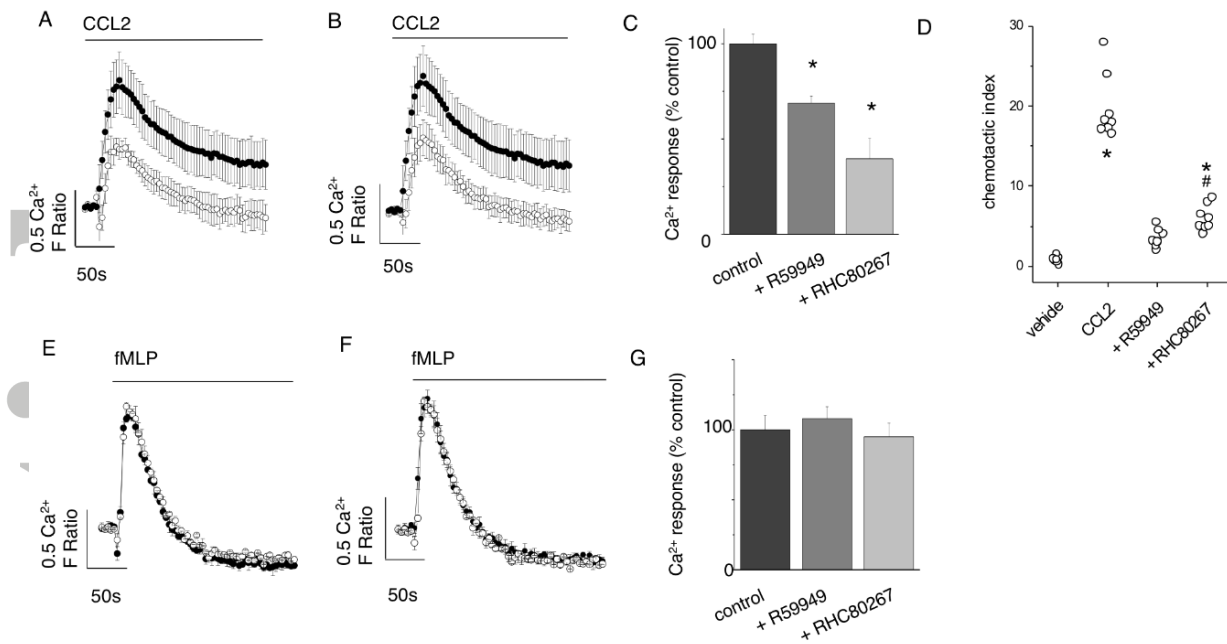
Figure 3 Responses to CCL2 but not fMLP are attenuated by DAG kinase and DAG lipase inhibitors in freshly isolated human monocytes. Effect of (A) DAG kinase inhibitor R59949 (30µM) and (B) DAG lipase inhibitor RHC80267 (30µM) on Ca^{2+} responses evoked by CCL2 (50 ng/mL) in monocytes (*N*=8). Averaged responses are shown in the presence of vehicle (*closed circles*) and inhibitor (*open circles*). (C) Bar chart showing effect of R59949 (30µM) and RHC80267 (30µM) on the peak Ca^{2+} response evoked by CCL2 (50 ng/mL) (*N*=8). (D) Effect of R59949 (30µM) and RHC80267 (30µM) on freshly isolated monocyte transmigration to CCL2 (3 ng/mL). * denotes *P*<0.05 versus vehicle and # denotes *P*<0.05 versus CCL2 alone (*N*=8). Lack of effect of (E) R59949 (30µM) or (F) RHC80267 (30µM) on Ca^{2+} responses evoked by fMLP (10 µM) in monocytes (*N*=6). Averaged responses are shown in the presence of vehicle (*closed circles*) and inhibitor (*open circles*). (G) Bar chart showing lack of effect of R59949 (30µM) and RHC80267 (30µM) on peak Ca^{2+} response evoked by fMLP (10 µM) (*N*=6). F ratio is the Ca^{2+} response as measured by the Fura-2 emission intensity ratio when excited at 340 and 380 nm. Data in inhibition experiments is expressed as a percentage of the control response in the presence of vehicle alone.
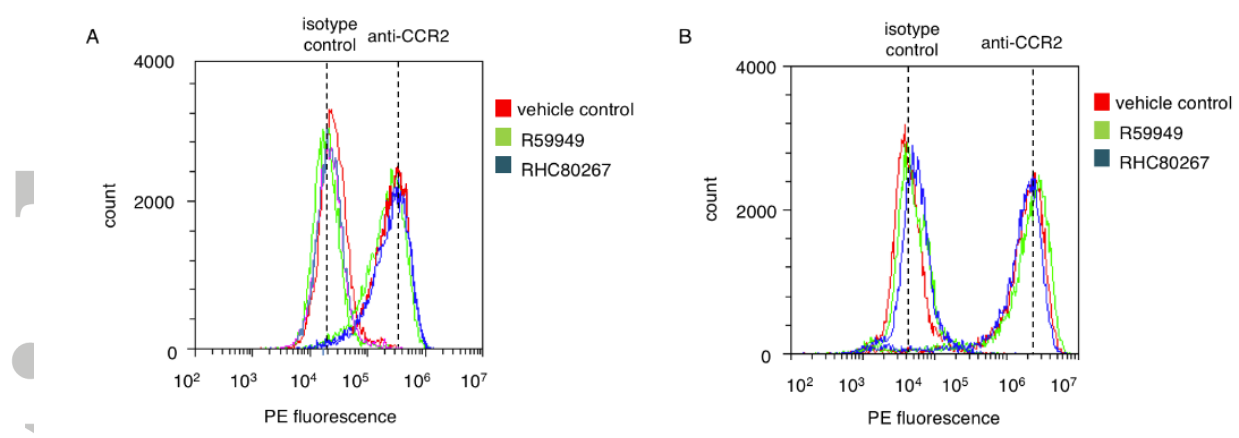
Figure 4 DAG kinase or DAG lipase inhibition does not reduced the cell surface population of CCR2 receptors in freshly isolated monocytes and THP-1 cells. 3 representative (N=6) flow cytometry profiles of freshly isolated CD14^{+} monocytes (A) and THP-1 cells (B) labelled with anti-CCR2 antibodies or isotype control. Cell are treated with vehicle control, R59949 (30µM) or RHC80267 (30µM). Anti-CCR2 cell surface immunoreactivity is indistinguishable between vehicle control and test groups.
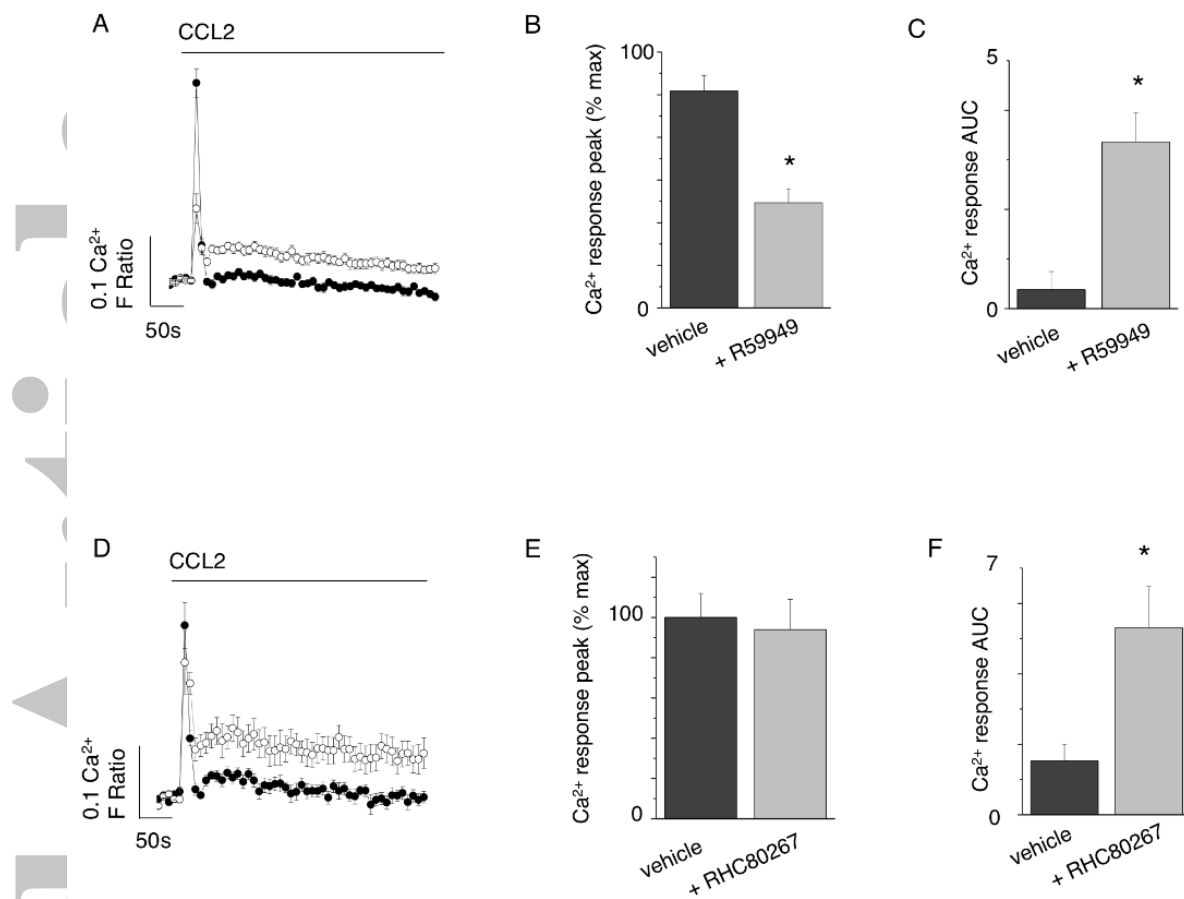
Figure 5 Effects of DAG kinase and DAG lipase inhibitors on CCL2-evoked Ca²⁺ responses in THP-1 cells in the absence of extracellular Ca²⁺. (A) Averaged (N=8) intracellular Ca²⁺ responses evoked by CCL2 (50ng/mL) in the absence of extracellular Ca²⁺ and presence (*open circles*) and absence *(closed circles)* of R59949 (30µM). (B) and (C) show the effect of R59949 on intracellular Ca²⁺ peak and area under the curve (AUC) in the absence of extracelluar Ca²⁺ (*N*=8). (D) Averaged (N=8) intracellular Ca²⁺ responses evoked by CCL2 (50ng/mL) in the absence of extracellular Ca²⁺ and presence (*open circles*) and absence *(closed circles)* of RHC80267 (30µM). (E) and (F) show the effect of R59949 on intracellular Ca²⁺ peak and AUC in the absence of extracelluar Ca²⁺ (*N*=8). * denotes *P*<0.05 versus vehicle control for all.
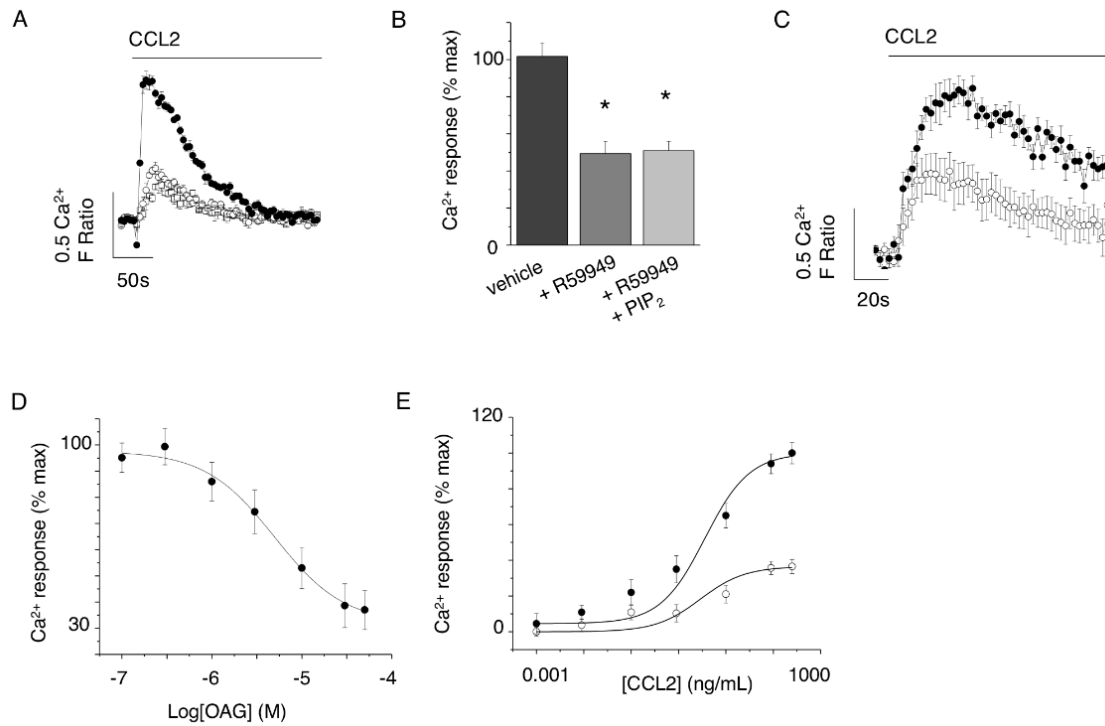
**Figure 6 Application of exogenous PIP₂ does not rescue CCL2-evoked Ca²⁺ response
following DAG kinase inhibition but inhibition is mimicked by OAG in THP-1 cells.** (A)
CCL2-evoked (50ng/mL) intracellular Ca²⁺ responses in the presence of vehicle control
(*closed circles*), R59949 (*open circles*; 30μM) or R59949 plus exogenous PIP₂ (*squares*;
300μM) (*N*=8). (B) Bar chart showing average peak intracellular Ca²⁺ responses. * denotes
P<0.05 versus vehicle control. (C) CCL2-evoked (50ng/mL) intracellular Ca²⁺ responses in
the presence of vehicle control (*closed circles*) or cell permeable DAG analogue, OAG (*open
circles*) (*N*=8). (D) Concentration-inhibition curve for OAG effect on intracellular Ca²⁺
responses evoked by CCL2 (50ng/mL) (*N*=8). (E) Effect of OAG (30μM) on CCL2
concentration-response curve in THP-1 cells (IC₅₀ 9±1μM; *N*=6). Responses are in the
presence of vehicle control (*closed circles*) or OAG *(open circles)*.   F ratio is the Ca²⁺
response as measured by the Fura-2 emission intensity ratio when excited at 340 and 380 nm.
Data in inhibition experiments is expressed as a percentage of the control response in the
presence of vehicle alone.
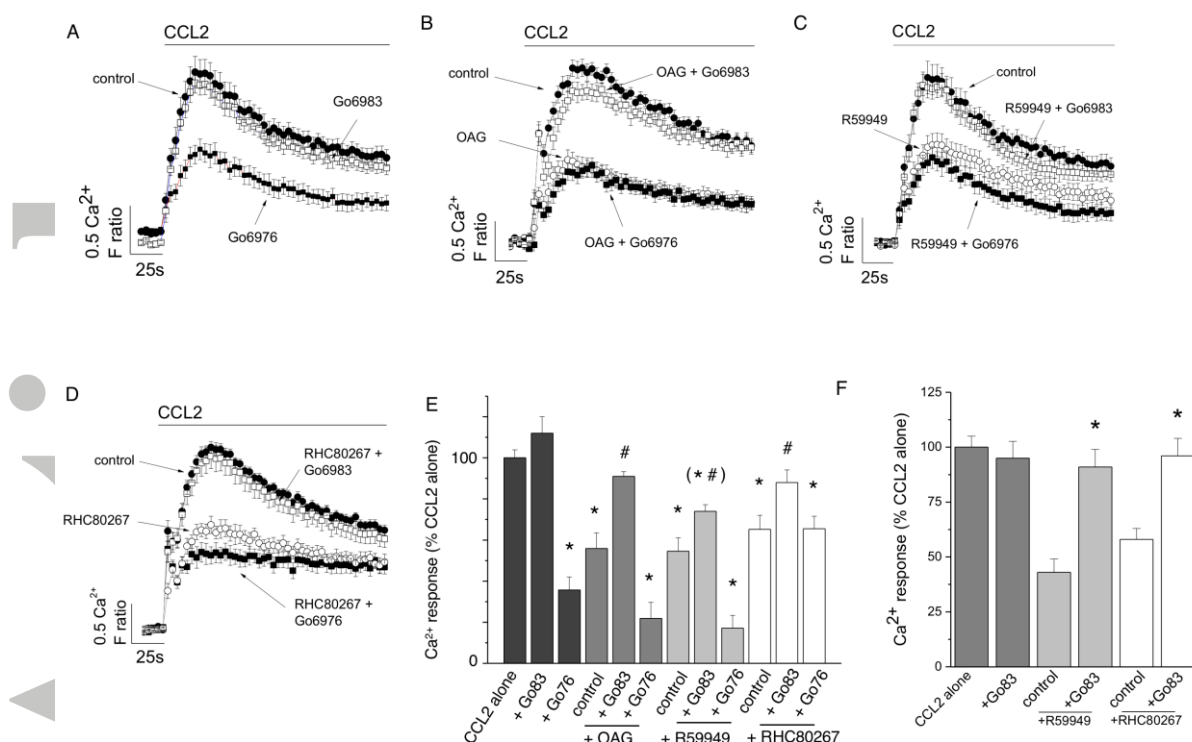
Figure 7 Effect of inhibiting Ca^{2+}-dependent and Ca^{2+}-independent PKC isoforms on CCL2-evoked responses following inhibition of DAG kinase and DAG lipase in THP-1 cells and freshly isolated monocytes. (A) CCL2-evoked intracellular Ca^{2+} responses in THP-1 cells the presence of vehicle control, Gö6976 (100nM) or Gö6983 (100nM) (N=8). (B) CCL2-evoked intracellular Ca^{2+} responses in THP-1 cells the presence of vehicle control and OAG (30μM) in the presence and absence of Gö6976 or Gö6983 (N=8). (C) CCL2-evoked intracellular Ca^{2+} responses in THP-1 cells the presence of vehicle control, and R59949 (30μM) in the presence and absence of Gö6976 or Gö6983 (N=8). (D) CCL2-evoked intracellular Ca^{2+} responses in THP-1 cells the presence of vehicle control, and RHC80267 (30μM) in the presence and absence of Gö6976 or Gö6983 (N=8). (E) Barchart showing averaged data from experiments (A-D). (F) Barchart showing CCL2-evoked Ca^{2+} responses in freshly isolated monocytes and the effect of R59949 (30μM) and RHC80267 (30μM), in the presence and absence of Gö6983 (100nM) (N=8). All intracellular Ca^{2+} responses are evoked by 50 ng/mL CCL2. * denotes P<0.05 versus CCL2 and # denotes P<0.05 for combined inhibitors over either OAG, R59949 or RHC80267 alone. F ratio is the Ca^{2+} response as measured by the Fura-2 emission intensity ratio when excited at 340 and 380 nm. Data in inhibition experiments is expressed as a percentage of the control response in the presence of vehicle alone.
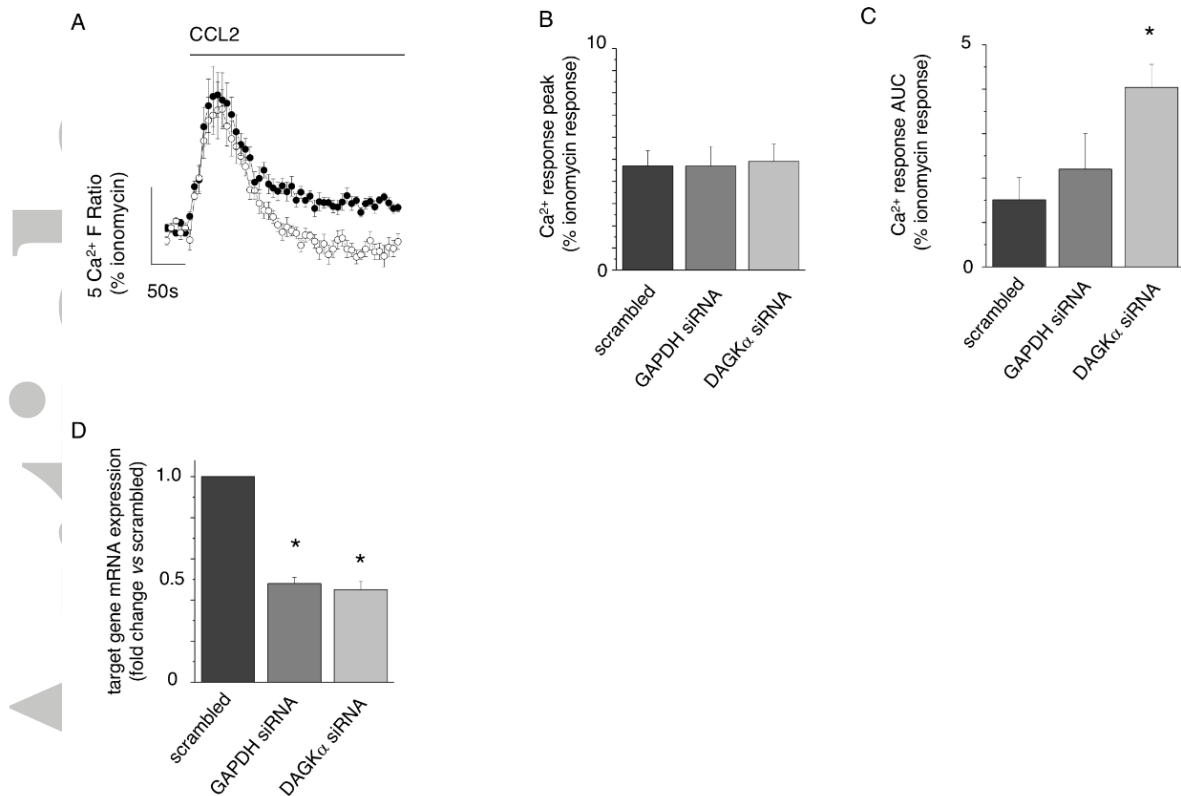
Figure 8 Effect of DAG kinase α knockdown of CCL2-evoked Ca^{2+} responses in THP-1 cells. (A) Averaged intracellular Ca^{2+} response evoked by CCL2 in THP-1 cells transfected with scrambled siRNA (*closed circles*) or DAG kinase alpha targeted siRNA (*open circles*) (*N*=8). Barcharts showing peak (B) and area under the curve (C) intracellular Ca^{2+} responses evoked by CCL2 in scrambled, GAPDH knockdown or DAG kinase alpha knockdown THP-1 cells (*N*=8). (D) qRT-PCR analysis of GAPDH or DAG kinase alpha mRNA transcripts in scrambled and knockdown THP-1 cells (*N*=8). F ratio is the Ca^{2+} response as measured by the Fura-2 emission intensity ratio when excited at 340 and 380 nm. Responses evoked by 50 ng/mL CCL2 for all experiments. * denotes *P*<0.05 versus scrambled control cells in all experiments. Data in each experiment is expressed as a percentage of the Ca^{2+} response to ionomycin to control of cell number in knockdown studies.

Table 1 Expression of DAG kinase, DAG lipase and PKC mRNA transcripts in CD14$^+$ monocytes and THP-1 cells. Data is representative of 5 donors/independent experiments. Sense and anti-sense primer sequences used for <mark>non-quantitative RT-PCR</mark> are given beneath each gene assayed. Positive control PCR products were generated for all primers sets using human brain cDNA template.

Gene	Name	CD14$^+$ monocytes	THP-1 cells
DGKA	**diacylglycerol kinase alpha**	expressed	expressed
Sense: Anti-sense:	CAACAGGAGGCAAAACTGGC TGCCACCTAGAGATCCACGA		
DGKB	**diacylglycerol kinase beta**	not expressed	not expressed
Sense: Anti-sense:	TCTGTGTGCAATGGAGGCAT CCACCCACAACAATCTGTCCA		
DGKD	**diacylglycerol kinase delta**	expressed	expressed
Sense: Anti-sense:	TTATTGGTTGCACGCACAGC CAGACCATCATCAAAGAGGGGA		
DGKE	**diacylglycerol kinase epsilon**	expressed	expressed
Sense: Anti-sense:	AGAGGGTAAGTCTCGTCCCC CTCTGGGAACAGGCAACGAT		
DGKG	**diacylglycerol kinase gamma**	expressed	expressed
Sense: Anti-sense:	GACTTCTCACCTGGCCTGTC GTCCCTCGGTCTTCAAGCTC		
DGKH	**diacylglycerol kinase eta**	expressed	expressed
Sense: Anti-sense:	TATCCCCAGATCCAGGCTGT CAGATGCAGCTATGCTCCCA		
DGKI	**diacylglycerol kinase iota**	not expressed	not expressed
Sense: Anti-sense:	TCCAGTGTGACATGGGCATC GGTACCTGAATCCACGGCAA		
DGKK	**diacylglycerol kinase kappa**	expressed	not expressed
Sense: Anti-sense:	CACTGGGCAATGCGATGATG TAACCAGACAAGCCCACGAC		
DGKQ	**diacylglycerol kinase theta**	expressed	expressed
Sense: Anti-sense:	AGGCTCCGAGAGTGACTGAT GTGAACCCCAAGAGTGGAGG		
DGKZ	**diacylglycerol kinase zeta**	expressed	expressed

Sense:	GGCTCAGGTCGAAGACTTGT		
Anti-sense:	CAGGATGCTGCAGAAGTCAGT		
DAGLA	**diacylglycerol lipase alpha**	expressed	expressed
Sense:	TGTCGGATGGCACAATGTCA		
Anti-sense:	GAGCCCAGGATGGAGGTGG		
DAGLB	**diacylglycerol lipase beta**	expressed	expressed
Sense:	GTTCGTACCACAAACCGTGC		
Anti-sense:	CTCCCAGGAAGCTGATCTGGA		
PRKCA	**protein kinase C alpha**	expressed	expressed
Sense:	CCTTTGCCACACACTTTGGG		
Anti-sense:	TGACCGAGTGAAACTCACGG		
PRKCB	**protein kinase C beta**	expressed	expressed
Sense:	TCTCTTGTCTCTAGCTTTTGGCT		
Anti-sense:	CCCGGAAGAAAAGACGACCA		
PRKCG	**protein kinase C gamma**	not expressed	not expressed
Sense:	TCTAGAATGGGACAGGGGGT		
Anti-sense:	CAGGACAGCCTCCCTTCGAT		
PRKCD	**protein kinase C delta**	expressed	expressed
Sense:	TGTTGAGGCCCCAGACAAAG		
Anti-sense:	TGGTGGTTGGTGCGTTGTAG		
PRKCE	**protein kinase C epsilon**	expressed	expressed
Sense:	GGTGCAGACTTGACACTGGT		
Anti-sense:	GAACCCGGCGAGGAAATACA		
PRKCH	**protein kinase C eta**	not expressed	expressed
Sense:	GATCCACCCAACCCTCGAA		
Anti-sense:	GCGGGGGTTCTGTGAACTTG		
PRKCQ	**protein kinase C theta**	expressed	expressed
Sense:	TTAAGCAGCGAGCCTGTTGA		
Anti-sense:	GAAACCTCAAGGCCGAATGC		
PRKCI	**protein kinase C iota**	expressed	expressed

Sense:	CCCTGGTGTTCATTGCCTCT		
Anti-sense:	GGCCTTTGCAATGAGGTTCG		

PRKCZ	**protein kinase C zeta**	expressed	expressed

Sense:	TGGCTTAAGGTCCTCCGAGT		
Anti-sense:	GAGTTCCGCGGAGTTGACC		